

Low-frequency Raman excitations in phase I of solid H₂: Role of crystal fields

Alexander F. Goncharov, Mikhail A. Strzhemechny,* Ho-kwang Mao, and Russell J. Hemley
*Geophysical Laboratory and Center for High-Pressure Research, Carnegie Institution of Washington,
 5251 Broad Branch Road NW, Washington, D.C. 20015*

(Received 17 March 2000; published 23 January 2001)

Low-frequency Raman spectra (up to 800 cm⁻¹) measured below 18 K are reported for the entire pressure range of phase I of para-hydrogen doped with low fractions of the ortho-modification. In addition to bands corresponding to the E_{2g} optical phonon and the $J=2\leftarrow 0$ rotational transitions, we observed a weak band attributed as $S_0(1)$. These spectra are employed to deduce information on the interactions that play a decisive role in bringing about the transition to the broken symmetry phase II. A new theoretical analysis is presented to understand the rotational Raman excitations and the role of various pairwise anisotropic interactions between H₂ molecules. In order to explain the pressure dependence of the $S_0(0)$ and $S_0(1)$ bands, we infer that a fourth-harmonic crystal field is present. The frequencies of the $S_0(0)$ and $S_0(1)$ bands are used to reconstruct the respective crystal field parameter.

DOI: 10.1103/PhysRevB.63.064304

PACS number(s): 62.50.+p, 63.20.Dj, 63.20.Kr, 77.80.Bh

I. INTRODUCTION

Solid hydrogen under high pressure has proved to be a fascinating and challenging subject of investigation. Our understanding of the numerous recent observations of high-pressure properties of the hydrogens is still far from the level achieved for low pressures.¹ Phase transitions at low temperatures to the broken-symmetry phases have been reported for the solids made up of the three stable hydrogen isotopes, in *o*-D₂ at 28 GPa,² in *p*-H₂ at 110 GPa,³ and in HD at 69 GPa.⁴ The electric quadrupole-quadrupole (EQQ) interaction plays a major, if not decisive, role as the agent that counteracts the kinetic energy and brings about those phase transitions. Therefore, an exact knowledge of this and other interactions involved is of primary importance for understanding the underlying physics of these phase transformations. A highly versatile and precise tool to obtain information on the interactions in the solid is Raman scattering. The first Raman experiments, reported in the early 1960s by Welsh and co-workers^{5,6} for solid *p*-H₂ at ambient pressure, revealed a great wealth of details on which, among others, the theory of solid hydrogen in its present-day form relies (see, for instance, Van Kranendonk¹). At high pressures, Raman spectra of *p*-H₂ were measured by the Silvera group first up to 54 GPa (Ref. 2) and then to 110 GPa.³ In this paper, we present high-resolution Raman measurements of the pure rotational bands in solid *p*-H₂ for pressures up to 110 GPa and provide a new interpretation. A preliminary report of some of the experimental data has already appeared.⁷

Throughout the range of phase I, the H₂ molecule mainly retains states of free rotors, and the relevant corrections to these states can be evaluated perturbatively. Thus, on the one hand, interpretation of experimental findings within this range remains comparatively simple; on the other hand, the compressions are high enough to bring about variations of the physical properties that enable coming to unambiguous conclusions about the main forces participating close to and across the phase transition line to phase II (see Ref. 8 for phase diagram). A remarkable fact was noticed⁹ that at high pressures the measured $S_0(0)$ bandwidth in the homonuclear

hydrogens^{2,3} is considerably narrower than could be expected if the quadrupoles were rigid and no other forces were present. Since the binding strength in the hydrogen molecule is very high, compression-related changes in the bond length should be small. Detailed evaluations show that it is so: the bond shortening and the pertaining changes of the quadrupole moment are indeed small (a few percent).⁹ This apparently weaker EQQ interaction was ascribed to a many-body screening,⁹ the effect of which can be taken into account by multiplying the EQQ parameter by the refractive index. We do not go into arguments concerning that model; rather, we suggest another cause behind that pressure-induced weakening of the EQQ interaction, as inferred from Raman frequencies.

The anisotropic interactions between hydrogen molecules include contributions other than EQQ (see, for instance, Ref. 1). At low pressures, the non-EQQ forces produce negligible effects; some of them are ineffective because of the high symmetry of both hcp and fcc phases. It is important that at higher pressures all the anisotropic interaction parameters must be exponential functions of the intermolecular distance R , whereas the EQQ parameter is proportional to R^{-5} . A simple and physically understandable way to account for the apparent weakening of the EQQ interaction is to assume that in the hcp lattice there is a crystal field of the form (referred to crystal axis c)

$$V_c(\mathbf{w}) = \epsilon_{4c} C_{40}(\mathbf{w}), \quad (1)$$

where $C_{40}(\mathbf{w})$ is Racah's spherical harmonic¹⁰ and \mathbf{w} denotes the orientation of the chosen molecule with respect to the c axis of the crystal. This term, which at high pressures originates mainly from Hartree repulsion, has been used to match theory and experiment for the $S_0(0)$ band even at zero pressure.¹¹ Presumably because of its smallness at zero pressure, it was later discarded in high-pressure evaluations. It should be noted that such a crystal field is responsible for the low-temperature zero-pressure thermodynamics of classical (cubic) rare-gas solids doped with rotor molecules.¹²

We also address here the problem of the second-harmonic crystal field components. In particular, we take into account one of the anisotropic interactions that has been ignored in the previous theories of the $S_0(0)$ band structure. Our analysis shows that the corresponding contribution might play an important role in the balance of anisotropic interactions, which determines the line separation in the $S_0(0)$ band.

The structure of the paper is as follows. In Sec. II we give the theoretical background needed for the interpretation and assignments (Sec. IV) of the experimental data presented in Sec. III. In Sec. V, our conclusions are formulated. Some numerical estimations are placed in the Appendices.

II. THEORETICAL BACKGROUND

The anisotropic, that is, orientation-dependent interaction between two hydrogen molecules can be represented as a sum of two terms,¹ one of which depends on the angular variables separately and the other, on both variables (the orientations are referred to the intermolecular axis):

$$V_{\text{anis}} = [A_1(\mathbf{w}_1) + A_1(\mathbf{w}_2)] + A_2(\mathbf{w}_1, \mathbf{w}_2), \quad (2)$$

where \mathbf{w}_i is the set of the angles that determine the orientation of molecule i .

The first two terms can be written as

$$A_1(\mathbf{w}) = B_2(R)C_{20}(\mathbf{w}) + B_4(R)C_{40}(\mathbf{w}). \quad (3)$$

Both anisotropic interaction terms have two contributions.¹ One of these, which is important at long distances, is due to the anisotropy of the polarizability of the hydrogen molecule. The other stems from the anisotropy of the electronic density which controls the so-called Hartree repulsion, or the valence forces. The function $B_2(R)$ has been evaluated^{1,13-15} based on potentials derived from first principles.¹⁴⁻¹⁶ Although $B_4(R)$ is expected on general grounds to be a strong function of the intermolecular distance R , especially at shorter ranges, little is known about $B_4(R)$; evaluation within the atom-atom approach for hydrogen is very unreliable.¹⁶ It was evaluated only for the equilibrium value of R at ambient pressure¹¹ to be small as compared to the respective EQQ contribution. An attempt to reconstruct this function¹⁷ from the *ab initio* potentials of Ree and Bender¹⁶ gave a negative B_4 within the range of our interest. The accuracy of that reconstruction is not high enough for our purposes.

The function $B_2(R)$ in Eq. (3) is appreciable even at zero pressure. However, because of the high symmetry of the hcp (or fcc) lattice, the term in Eq. (3) vanishes completely when summed over all the neighbors, unless the lattice parameter ratio c/a is different from its ideal value of $\sqrt{8/3}$. Taking into account only nearest neighbors at R_δ , we have¹

$$\epsilon_{2c} \approx \sqrt{6} \delta_c \tilde{B}_2(R_\delta), \quad (4)$$

where $\delta_c = c/a - \sqrt{8/3}$ and

$$\tilde{B}_2(R) = B_2(R) + \frac{1}{2} R \frac{dB_2}{dR}. \quad (5)$$

By contrast, the fourth-harmonic interaction does not cancel out upon summation over neighbors but yields the field of Eq. (1) with $\epsilon_{4c} = (7/6)B_4(R_\delta)$, if only nearest neighbors are taken into account.

The last term in Eq. (2), which depends on both angular variables, comprises three components. In addition to the two contributions of similar nature (valence and induction-dispersion) as in Eq. (3), this term includes an electrostatic contribution caused by the intramolecular distribution of charges of both signs. This interaction is controlled by operators of the quadrupole moments of both interacting molecules. Since in this paper we concentrate on Raman spectra of p -H₂, of the last term in Eq. (2) we leave only the site-off-diagonal hopping Hamiltonian, which in the most general form can be written as (we use the standard notation for the scalar and direct products of two irreducible tensors¹⁰)

$$V_{20}(\mathbf{w}_1, \mathbf{w}_2) = \sum_{L=0,2,4} \epsilon_L^{02}(R) \{ \mathbf{C}_2(\mathbf{w}_1) \otimes \mathbf{C}_2(\mathbf{w}_2) \}_L \cdot \mathbf{C}_L(\mathbf{n}) \quad (6)$$

with \mathbf{n} being the unit vector along the intermolecular axis. The origin of the parameters $\epsilon_L(R)$ are the same as in the analog of Eq. (6) for directly interacting $J=1$ molecules (see, e.g., Ref. 1). The superscript 02 implies that the matrix elements of the quadrupole moment of both interacting molecules are taken between the rotational states $J=0$ and $J=2$. In particular, the parameter $\epsilon_4^{02}(R)$ is predominantly of EQQ nature, at least at low pressures. The parameter $\epsilon_2^{02}(R)$ [as well as the non-EQQ part of $\epsilon_4^{02}(R)$] originate from valence forces. The parameter $\epsilon_0^{02}(R)$ is of little importance for our purposes because it does not make the $S_0(0)$ line split.

The EQQ part of $\epsilon_4^{02}(R)$ can be written as

$$\epsilon_4^{02}(R) = \sqrt{70} \frac{q_{20}^2}{R^5}, \quad (7)$$

where $q_{20} = \langle 2 | \hat{Q} | 0 \rangle$ is the adiabatic matrix element of the electrical quadrupole moment operator \hat{Q} between purely rotational states with $J=0$ and $J=2$. Since the matrix element q_{11} , which appears in the direct EQQ interaction of two $J=1$ molecules, differs negligibly^{1,18} from q_{20} , in our considerations we can use the well known EQQ interaction parameter

$$\Gamma = \frac{6}{25} \frac{q_{11}^2}{R^5}. \quad (8)$$

In our examination of the high-pressure Raman spectra, we wish to know what effects will be due to the various Hamiltonian terms. One should note that the direct products in the Hamiltonian of Eq. (6) are irreducible tensors of the respective ranks and thus each of them, by virtue of the Wigner-Eckart theorem, will produce splittings with the same spacing ratios as the respective crystal fields. The term with $L=0$ is a scalar and therefore can lead only to a general lowering of the center of gravity of the entire band. The term

with $L=2$ is a rank-2 tensor and thus will produce splittings with the same spacing ratio as the crystal field originated from the rank-2 term in Eq. (3). Similarly, the splittings will be the same due to the rank-4 crystal field and the hopping interaction of Eq. (6). It is important that $\epsilon_4^{\text{non}Q}$, being also positive like Γ , can only increase the strength of this rank-4 contribution. Normally, *ab initio* calculations^{14–16} give the aggregate parameter $\epsilon_4(R)$, from which the EQQ contribution can be separated.¹

We will need some spectra in the crystal fields of ranks 2 and 4. The rank-4 crystal field of Eq. (1) will produce the following levels $E_4(2m)$ for the $J=2$ state:

$$E_4(2m) = \frac{1}{21} \epsilon_{4c} A_4(2m);$$

$$A_4(20) = 6; A_4(2\pm 1) = -4; A_4(2\pm 2) = 1. \quad (9)$$

Similarly, for the $J=3$ state in the same crystal field

$$E_4(3m) = \frac{1}{33} A_4(3m);$$

$$A_4(30) = 6; A_4(3\pm 1) = 1;$$

$$A_4(3\pm 2) = -7; A_4(3\pm 3) = 3. \quad (10)$$

For the sake of completeness we also give the levels for the $|2m\rangle$ and $|3m\rangle$ states in a rank-2 crystal field with the strength parameter ϵ_{2c}

$$E_2(2m) = (1/7) \epsilon_{2c} A_2(2m);$$

$$A_2(20) = 2; A_2(2\pm 1) = 1; A_2(2\pm 2) = -2 \quad (11)$$

and, similarly,

$$E_2(3m) = (1/15) A_2(3m);$$

$$A_2(30) = 4; A_2(3\pm 1) = 3;$$

$$A_2(3\pm 2) = 0; A_2(3\pm 3) = -5. \quad (12)$$

We recapitulate the results of the known theory^{11,19} for the purely rotational Raman band $S_0(0)$, which will be useful for our purposes at high pressures. The Raman frequencies of the $J=2$ roton excitations (expressed in our notation), if only nearest neighbors are taken into account, are

$$\nu_m[S_0(0)] = \nu_g[S_0(0)] + \Delta\nu + A_4(2m) \left\{ \frac{7}{6} \epsilon_4^{02} + \frac{1}{21} \epsilon_{4c} \right\}$$

$$- \frac{1}{7} A_2(2m) \epsilon_{2c}. \quad (13)$$

Here $A_4(2m)$ are as in Eq. (9) and $A_2(2m)$ as in Eq. (11); ν_g is the unsplit free-molecule value of the $S_0(0)$ line frequency; $\Delta\nu$ represents a sum of spectroscopic corrections which can be pressure dependent but do not cause the line to split. It is important that both of these rank-4 irreducible tensors produce three lines that are separated equidistantly. It should be also remarked that the contributions of the second-harmonic crystal field to the line splitting are highly (1:3) nonequidistant. At zero pressure, the second term in the curly brackets of Eq. (13) amounts to about 2% of the first term. Presumably because of this smallness and lack of knowledge, this term was simply omitted in later interpretations of

high-pressure Raman data. Since this term is expected, on general grounds, to be a strong exponential function of R at short ranges, we reinvoked its use at high pressures.

Unfortunately, the term of rank-2 with $L=2$ in Eq. (6) was disregarded in earlier theory, although its strength might be comparable to that of the rank-2 crystal field. We correct this deficiency. The calculation can be done as outlined by Van Kranendonk.¹⁹ The respective contribution to the Raman spectrum to be added to the last term of Eq. (13) is

$$\frac{\sqrt{6}}{2} \delta_c \tilde{\epsilon}_2 A_2(2m), \quad (14)$$

where, similarly as in Eq. (4),

$$\tilde{\epsilon}_2 = \epsilon_2 + \frac{1}{2} R \frac{d\epsilon_2}{dR}. \quad (15)$$

We note that this term and the one associated with ϵ_4^{02} in Eq. (13) are off-diagonal contributions, as opposed to diagonal terms, scaled by ϵ_{4c} and ϵ_{2c} in Eq. (4).

III. EXPERIMENTAL RESULTS

We present here the results of a series of Raman measurements in p -H₂ in the pressure range 2–73 GPa at temperatures 4–8 K. We converted the sample from normal hydrogen by holding it for 100 h at 10 K at 33 GPa, utilizing the large increase of conversion rates under pressure.⁸ We monitored the intensity of the rotational Raman and infrared (IR) bands as a function of time (as in Refs. 8 and 20) to ensure the high extent of conversion. Then the pressure was increased to 73 GPa at low T and subsequently released to 2 GPa. At this pressure, the $S_0(0)$ and $S_0(1)$ excitations look like narrow unperturbed bands³ and the ortho concentration c can be reliably determined from intensity ratios of those bands. We found c to be about 2%. The Raman and IR data obtained in this series together with the previously published data^{8,20} constitute a complete set for the p -H₂ in phase I up to the transition to phase II (BSP phase) at 110 GPa.^{3,20} We used high-purity low-fluorescence synthetic diamonds as a material for the high-pressure windows. The high-pressure Raman details can be found in Ref. 21. The experimental technique has been published elsewhere.^{7,8} In this paper we address the Raman excitations up to 800 cm⁻¹, specifically the pure rotational transitions.

In Fig. 1 we show representative spectra of the $S_0(0)$ band at selected pressures. At lower pressures ($P < 10$ GPa) the E_{2g} phonon does not affect the well-resolved $J=2 \leftarrow 0$ triplet. With increasing pressure, the optical phonon begins to interact with the $m = \pm 2$ feature. After the phonon passes through the interaction region, the $S_0(0)$ band again exhibits a well resolved triplet. This was treated previously in terms of a Fermi-resonance interaction in pure ortho and para samples as well as mixed crystals.^{2,20} As the pressure is further increased approaching the critical value (I - II transition), the uppermost line spreads and decreases in intensity.

Since our samples contained a small concentration of ortho species we saw weaker bands at around 600 cm⁻¹ and

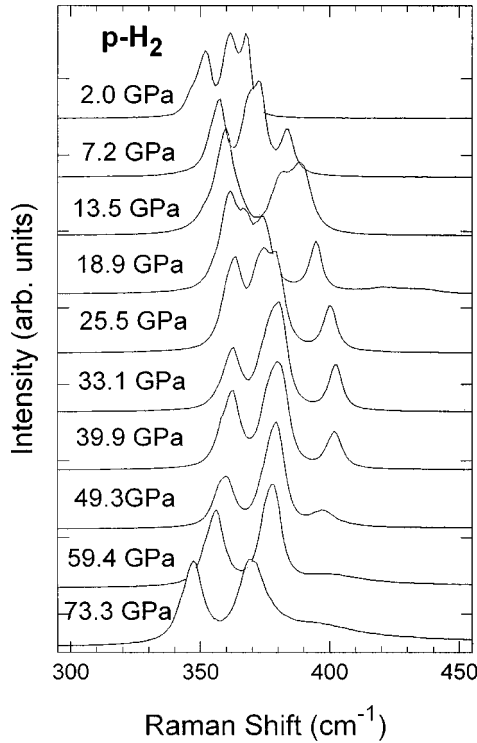


FIG. 1. Representative spectra showing evolution of the $S_0(0)$ band with pressure.

higher; judging from their positions and intensities, we attribute them to the $J=3 \leftarrow 1$ transitions [$S_0(1)$ line]. This line is well observed in ortho-rich systems at ambient⁶ or high²⁰ pressures. To our knowledge, measurements involving this band in almost pure p -H₂ have not been reported previously. Figure 2 shows part of the Raman spectra recorded at pressures from 2 to 50 GPa. One can see that this band is split in two features of unequal intensities and widths. At pressures above 30 GPa a stronger line belonging to the E_{2g} optical phonon emerges. The phonon appears to interact with only the upper, sharper feature.

In Fig. 3 we present the pressure dependence of the Raman frequencies in this range, including the pure rotational bands $S_0(0)$ and $S_0(1)$ as well as the E_{2g} phonon. The frequencies of the $S_0(0)$ band and E_{2g} phonon are in good agreement with Refs. 2 and 3. One can see that the lines related to the ± 1 and ± 2 sublevels of the $S_0(0)$ band seem to be split. A similar splitting has been observed previously.² The origin of this splitting is not clear but most likely it is due to residual shear strains present in the samples.

The most notable feature is the rapid increase of the splitting of $S_0(1)$ with pressure (Fig. 2). The broad low-energy feature belonging to the $S_0(1)$ band is shown in Fig. 3 as a single line. We did not try to resolve it further into smaller components, although there is possible evidence for additional structure.

IV. ANALYSIS AND DISCUSSION

To interpret the new Raman data we recall that important information is contained in the level splitting ratio of the

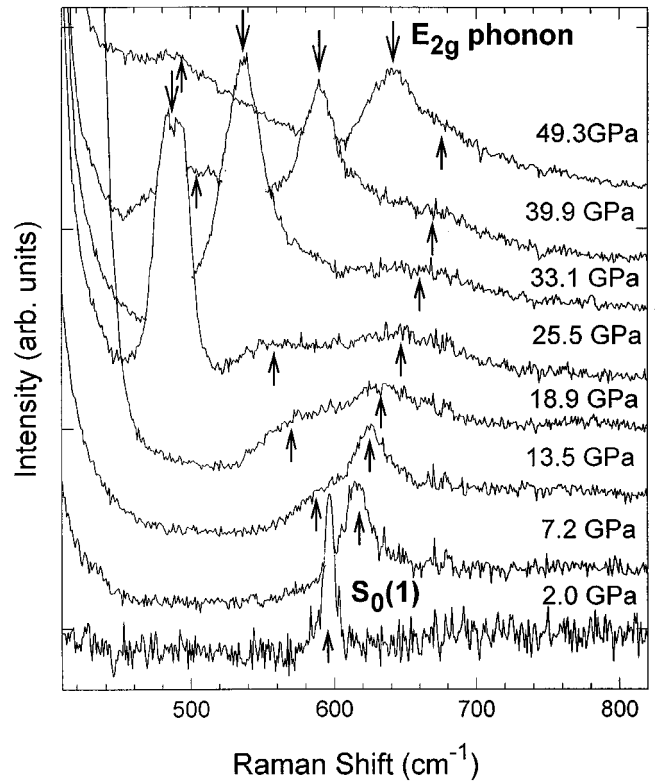


FIG. 2. Spectral range showing lines attributed to the $J=3 \leftarrow 1$ transitions. The E_{2g} phonon, indicated by the downward arrow, appears at about 10 GPa, shifting with pressure to higher energies.

$S_0(0)$ band. The two Raman splittings, $\nu(2,0) - \nu(2, \pm 2)$ and $\nu(2, \pm 2) - \nu(2, \pm 1)$, are plotted as a function of pressure in Fig. 4. If the line could be resolved into two components, we took an average of the two. At pressures roughly from 10 to 25 GPa the E_{2g} optical phonon interacts strongly with the middle ($2, \pm 2$) mode and destroys the balance between the level spacings. Outside this range to within the experimental uncertainty, which might be due to the same cause as the subcomponent splitting, the splittings are virtually equal implying that the second-rank field is weak. The fast decrease of the $J=2, m=0$ Raman line might be indicative of a depletion owing to the admixture of this state to the nominal $J=0$ state from which the roton is Raman excited.

Employing the measured equation of state,²² we plot all the splittings together in Fig. 5 as a function of the density ratio (compression) $\xi = \rho/\rho_0$ and fit these aggregate data to a polynomial function. We also show what one would expect if the splitting followed the dependence characterized by the EQQ-like rank-4 anisotropic interaction, described by the interaction parameter $\varepsilon_4(R)$ in Eq. (6) as calculated from first principles.¹⁵ As first noted by Loubeyre, Jean-Louis, and Silvera,⁹ at relatively moderate pressures, the splittings are roughly consistent with the EQQ dependence but at higher pressures start to deviate strongly. If we assume that these deviations are caused by the ever increasing fourth-harmonic crystal field, then we can deduce its magnitude by subtracting the fitting curve(s) from the expected dependence of ε_4 on R (or ξ). To translate those deviations into the crystal field terms, we multiply the discrepancy by 21/5; the result is

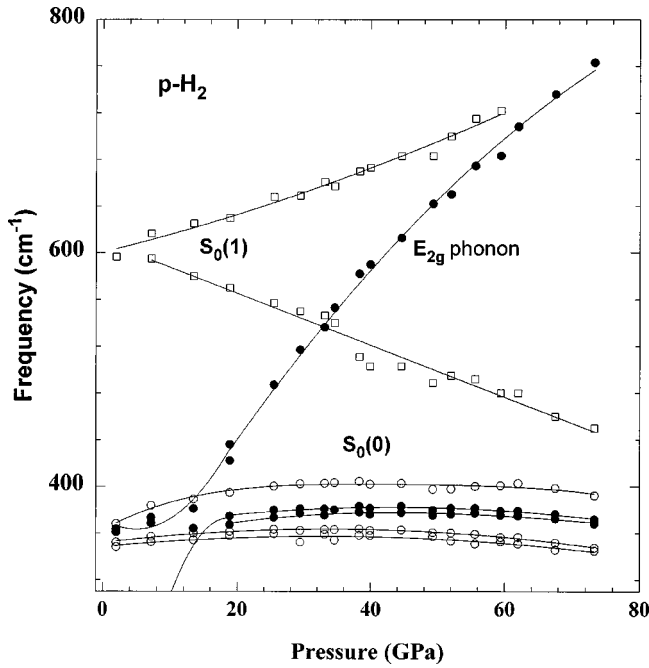


FIG. 3. The low-lying Raman frequencies vs pressure. Notice the mixing and repulsion of the terms of the same symmetry, the S_{2g} phonon, and the $m = \pm 2$ feature of $S_0(0)$.

plotted in Fig. 6. We also show the values reconstructed by Aviram, Goshen, and Thierberger¹⁷ from the calculations of Ree and Bender.¹⁶ As known, interactions between any two hydrogen molecule species are basically the same. Crude evaluation of the same rank-4 crystal field in D_2 from the available data in graphical form² yields, taking into account different spacings and quadrupolar moments, virtually the same result as shown in Fig. 6.

Now we evaluate the second-rank crystal field contribution. If we assume that only the diagonal rank-2 crystal field

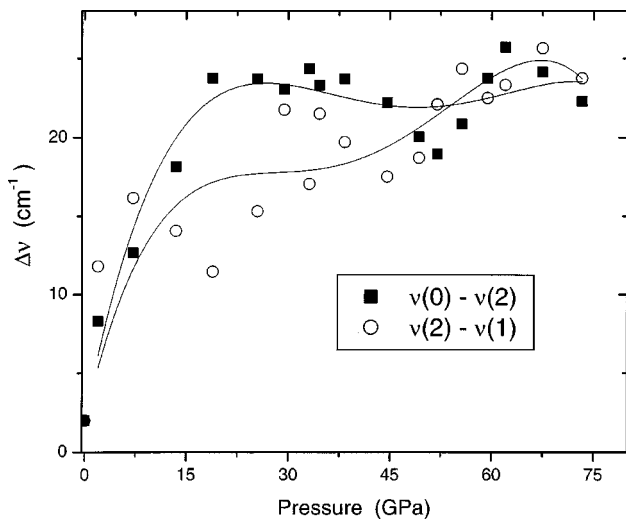


FIG. 4. The level difference for the $S_0(0)$ triplet as a function of pressure. Notice the substantial deviations from equidistance within the range of strong interaction with the E_{2g} phonon. The curves are polynomial fits.

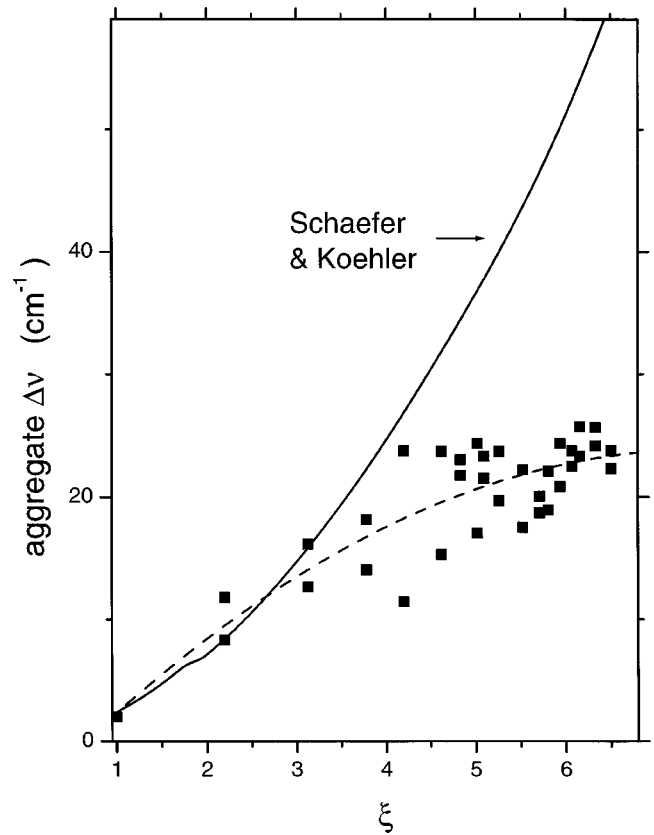


FIG. 5. The splittings of the $S_0(0)$ band as a function of the density ratio. The dashed curve is an aggregate polynomial fit. The solid curve is the splitting value from the *ab initio* anisotropic potential term ϵ_4 of Schaefer and Köhler (Ref. 15).

is effective, then from Eqs. (11) and (13) it follows that the relevant parameter ϵ_{2c} is exactly equal to the difference between the upper and lower splittings of the $S_0(0)$ triplet. We show this difference (ϵ_{2c}) in Fig. 7. The 10–35 GPa range may be treated as unreliable for reconstructing the ϵ_{2c} values because here the E_{2g} phonon distorts strongly the balance between the splittings. For example, at 73.3 GPa we have $\epsilon_{2c} = -1.45 \text{ cm}^{-1}$. From the V_{202} potential value of Schaefer and Köhler¹⁵ we calculate for the corresponding intermolecular distance of 3.8 a.u. $\tilde{B}_2 \approx -176 \text{ cm}^{-1}$ to reconstruct using Eq. (4) a net $\delta_c = 3.4 \times 10^{-3}$. This is roughly an order of magnitude less than the maximum absolute deviation δ_c (but of opposite sign) found at room temperature at the same pressure.²³ On the other hand, this estimate is reasonably consistent with the trend revealed in the low-temperature structure measurements at much lower (below 2.5 GPa) pressures.²⁴ The c/a ratio has not been determined for $p\text{-H}_2$ at low temperatures and high pressures; pressure-induced changes in δ_c may be expected on theoretical grounds.^{25,26} The general view of the crystal field spectra for both ranks 2 and 4 have much in common. If we ascribed the remaining part of the splitting to a rank-2 crystal field with (see above) $\tilde{B}_2 \approx -176 \text{ cm}^{-1}$, we would have $\delta_c > 0$ and close to 0.3. Such a huge *elongation* of the elementary cell would have resulted in splittings of the $J=2$ roton of over 150 cm^{-1} .

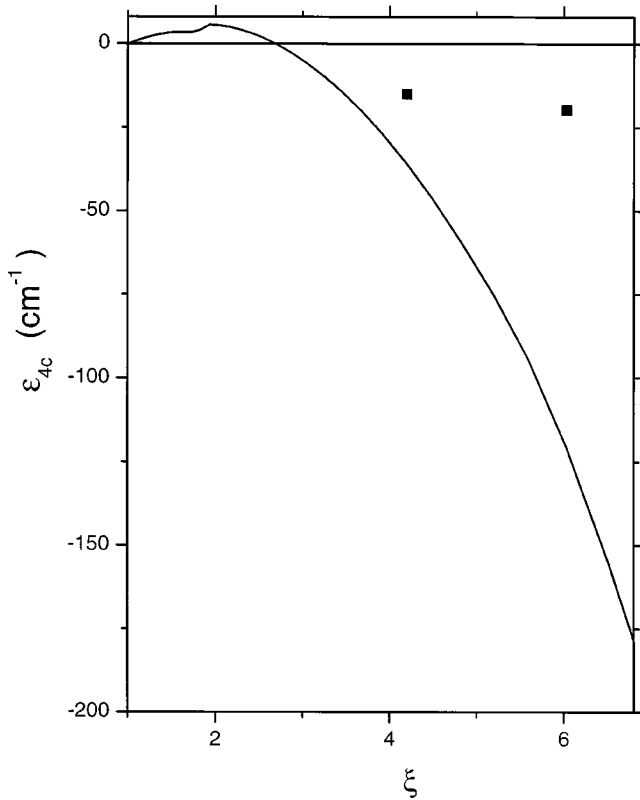


FIG. 6. The rank-4 crystal field parameter ϵ_{4c} vs compression ξ . The squares are estimates from Aviram, Goshen, and Thierberger (Ref. 17).

We can apply the conclusions drawn so far to the $S_0(1)$ band. We recall that in our experiments the ortho fraction was low (roughly 2%, see above). Hence, the Raman transitions must be virtually independent events occurring on iso-

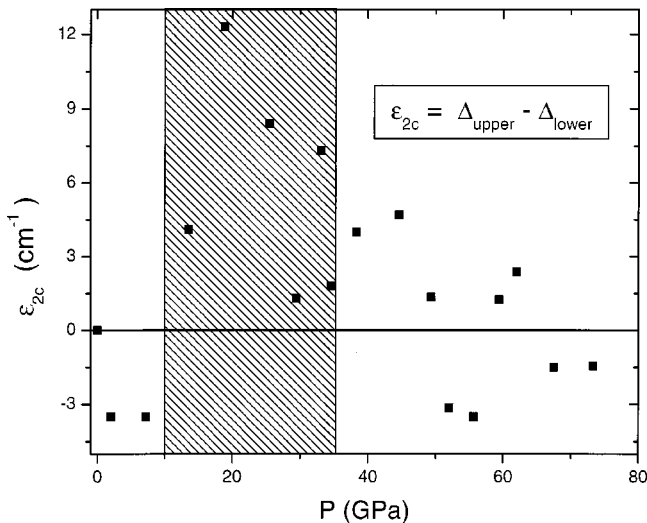


FIG. 7. The net rank-2 crystal field parameter as deduced from $S_0(0)$ splittings in Fig. 4 vs pressure. The shaded area is the range where the E_{2g} phonon strongly mixes with the $J=2; m=\pm 2$ states. We stress that, considering the relatively large uncertainty at higher pressure of about $3\text{--}4\text{ cm}^{-1}$, this plot is experimental evidence that the rank-2 contribution is small.

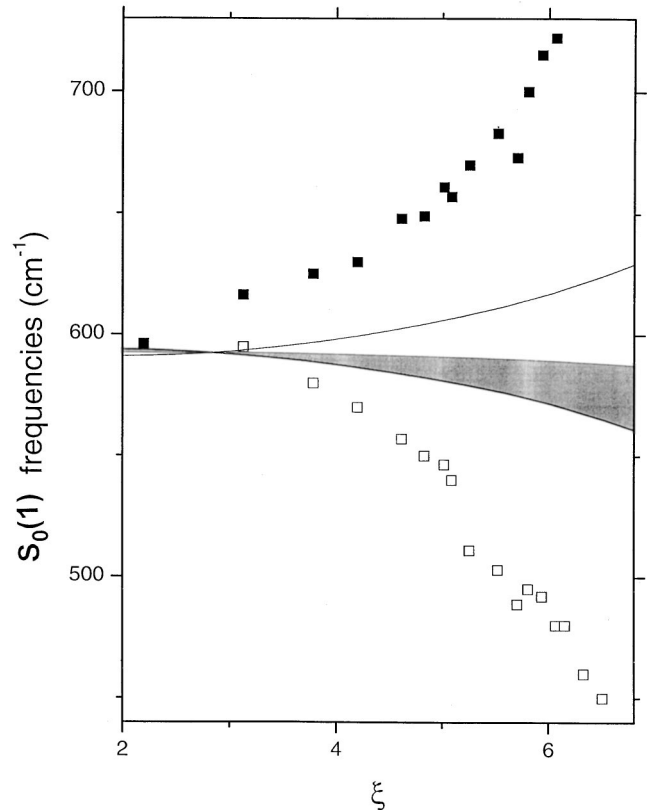


FIG. 8. The $S_0(1)$ Raman spectrum as a function of compression ξ . The lower three of the calculated lines are shown as a broad unresolved (shaded) band. Theory gives 25%–40% of the actual splitting.

lated $J=1$ centers (or pairs). The final $J=3$ state cannot hop on adjacent sites occupied by para molecules and thus is not broadened into a band like the $J=2$ roton. If we assume that the ortho molecules are singles, then the relevant spectrum is given by Eq. (10) with the crystal field parameter shown in Fig. 6. Since the field is *negative*, the uppermost level belongs to the $m=\pm 2$ states, which can interact with the E_{2g} phonon. From Eq. (10) one can easily notice that the other three levels stand off the $m=\pm 2$ line, forming a group of five closely spaced states with the center of gravity at $14/5$ in the units of Eq. (10). Thus, if our reasoning is correct, the $J=3\leftarrow 1$ line must appear as a doublet with the high frequency feature being noticeably narrower than the lower one unless the phonon line is close. This agrees qualitatively with the character of the spectra in Fig. 2. Using the ϵ_{4c} values deduced from the $S_0(0)$ band (see Fig. 6) we compare calculated line positions with the experiment in Fig. 8. One can see that the theory based on the deduced rank-4 crystal field parameter gives a fully consistent description (sign and order of magnitude) of the Raman spectrum of the $J=3\leftarrow 1$ transitions. However, the strength of the crystal field seems to be insufficient (by a factor of approximately 3–3.5) to account for the splitting observed. The reason behind this discrepancy is not clear but we point out that δ_c is not known experimentally for $p\text{-H}_2$ at these temperatures.

We have considered a few possible causes of the above inconsistency. In particular, we evaluated (see Appendices A

and B) the effect on the spectra of solitary $J=3$ states of the renormalization due to (i) the rank-4 crystal field itself and (ii) the “rotational induction” around an ortho impurity for a pressure of 73 GPa. As one can see the correction of the first type is below 1%. The rotational induction corrections are somewhat larger but small enough to justify the perturbative approach. We do not expect stronger effects for much higher pressures. At the same time, we must add that the rotational induction seems to be the main source of the compression-related shifts of the centers of gravity of the rotational levels. Since these effects for $J=3$ and $J=1$ levels are of opposite signs, the calculated positive shift ($\sim 13 \text{ cm}^{-1}$) of the mean $S_0(1)$ energy is of correct magnitude (see Figs. 3 or 8).

There is another possible reason behind the quantitative mismatch for the $J=3 \leftarrow 1$ energies between experiment and the theory based solely on the rank-4 crystal field. The point is that both anisotropic interaction parameters $B_2(R)$ in Eq. (3) and $\varepsilon_2(R)$ in Eq. (6), especially at close ranges, are still uncertain. *Ab initio* calculations give the respective interaction potential terms with different signs (compare ε_2 in Refs. 1, 14, and 15). Hence one might suppose that these two rank-2 contributions cancel one another in the $S_0(0)$ spectra. However, since the molecular-field term is not operative at isolated ortho centers they feel the action of the uncompensated rank-2 crystal field adds up to the splitting effect of the rank-4 crystal field discussed in detail in the present paper.

V. CONCLUSIONS

We have measured low-frequency Raman spectra of phase I of solid $p\text{-H}_2$ containing a low fraction of the ortho modification. The behavior of the $S_0(0)$ band is in good agreement with the previous experimental findings. We have observed a weak $S_0(1)$ band, which splits into two features of unequal width as the pressure increases. We suggest a new interpretation for the apparent inconsistency of the EQQ interaction to account for the splitting of the $S_0(0)$ Raman band as arising from a fourth-harmonic crystal field. The respective anisotropic potential component $V_{404}(R)$, reconstructed from the $S_0(0)$ data, is negative in sign and has the correct magnitude for describing qualitatively the spectrum of $J=3 \leftarrow 1$ transitions on isolated ortho molecules. Our theory accounts for approximately 30% of the observed level splitting and the contribution due to the lattice parameter deviation $\delta_c = c/a - \sqrt{8/3}$ was examined. Because its sign is opposite to that of the EQQ interaction, the rank-4 crystal field counteracts the effect of the latter, as it is with the frequencies of the Raman-active $J=2$ excitations. A similar consequence can manifest itself in shifting the pressure of transition to phase II to appreciably higher values than predicted by EQQ calculations. All the inferences and evaluations concerning the rank-4 crystal field are fully applicable to solid D_2 and, to a lesser extent HD, taking into account different quadrupolar moments and intermolecular distances.

ACKNOWLEDGMENTS

We are grateful to J. F. Shu for help with the experiments, and to NSF (Grant No. DMR-9972750) and NASA for support.

APPENDIX A

Actually, all spectra calculated in Sec. II are first approximation values in the respective crystal fields. For an isolated $J=3$ state the spectrum of the first approximation in the rank-4 crystal field V_4 is given in Eq. (10). Here we calculate corresponding second-order corrections. The Hamiltonian of this eigenvalue problem $H=T+V_4$ (T is the kinetic energy) mixes states of the same parity, odd in this particular case. We will take into consideration the levels $J=1$ and $J=3$, not needing to address higher- J levels because of the large kinetic energy difference. The Hamiltonian H conserves the magnetic number m and, therefore, the problem can be solved for every m separately. The wave function ψ for a given m is a linear combination: $\psi(m) = a_m|1m\rangle + b_m|3m\rangle$. The Schrödinger equation $H\psi(m) = E\psi(m)$ produces the following set of equations for a and b (we omit for the time being the index m , the same for all the quantities involved)

$$2Ba + V_{13}b = Ea;$$

$$V_{13}a + (12b + V_{33})b = Eb, \quad (\text{A1})$$

where $V_{13}(m) = \sqrt{7/3}C(431;00)C(431;0m)$ with $C(431;0m)$ being the Clebsch-Gordan coefficients; B is the rotational constant; and $V_{33}(m)$ are the energies in Eq. (10). The set Eq. (A1) produces a quadratic equation which can be easily solved analytically. Making use of the potential values,¹⁵ we estimate for $\xi = 6.5$ (or $P = 73$ GPa) the largest relative corrections (for $m=0$) to be -2.6% for level (1,0) and $+0.4\%$ for level (3,0).

APPENDIX B

The para neighbors of the single ortho molecule impurity feel the orienting action of the quadrupole at the impurity site. In virtue of the conclusions drawn in Appendix A we do not need to consider higher rotational levels. Now the Hamiltonian is (we leave the strongest, EQQ interaction)

$$H = T_0 + \sum_j T_j + \sum_j \hat{V}_Q(0,j), \quad (\text{B1})$$

where T_j is the kinetic energy of para neighbor j and $V_Q(0,j)$ is the EQQ-related interaction in Eq. (V02) between molecules at sites 0 (occupied by the ortho impurity) and j . There are no nonzero diagonal matrix elements between the $J=0$ and $J=3$ states; hence, we calculate the corrections to second order. This means that all corrections are of the same sign for all sublevels.

The effective Hamiltonian arises from terms that are diagonal in $J_0=3$ and off-diagonal in J_i of para molecules at sites i ; thus we obtain

$$H_{\text{eff}} = \sum_{j,(\text{int})} \frac{\hat{V}_Q(j)|\text{int}\rangle\langle\text{int}|\hat{V}_Q(j)}{E(3m) - E(2n)}. \quad (\text{B2})$$

The sum runs over para neighbors and excited states; $E(Nn)$ denotes the energies of the sublevels involved; $|\text{int}\rangle$ is the intermediate excited state with neighbor j in the $J=2$ state. If

we ignore the sublevel difference for the $J=2$ level, we can put $E(2n)=6B$ and sum up over intermediate states by closure. This yields an effective Hamiltonian proportional to a product of two rank-2 operators, $C_{2\nu}(\mathbf{w}_0)C_{2\nu'}(\mathbf{w}_0)$, that acts on the angular variables of the ortho impurity. This result can be represented as a sum of irreducible tensors of ranks 0, 2, and 4. The rank-0 operator is the global shift of the $J=3$

level, and this shift is the major consequence of this rotational induction effect. Our estimates show that at $\xi=6.5$ ($P\approx 73$ GPa) the center of gravity of the $J=3$ level shifts upward by 5.6 cm^{-1} . At the same time, the rank-4 component of the effective Hamiltonian leads to a splitting increase of 0.24 cm^{-1} , which amounts to 0.4% of the rank-4 crystal field splitting.

*Permanent address: Verkin Institute for Low Temperature Physics and Engineering, 47 Lenin Ave., Kharkov 310164, Ukraine.

¹J. Van Kranendonk, *Solid Hydrogen* (Plenum, New York, 1983).

²I.F. Silvera and R.J. Wijngaarden, *Phys. Rev. Lett.* **47**, 39 (1981).

³H.E. Lorenzana, I.F. Silvera, and K.A. Goettel, *Phys. Rev. Lett.* **64**, 1939 (1990).

⁴F. Moshary, N.H. Chen, and I.F. Silvera, *Phys. Rev. Lett.* **71**, 3814 (1993).

⁵H.P. Gush, W.F.J. Hare, E.J. Allin, and H.L. Welsh, *Can. J. Phys.* **38**, 176 (1960).

⁶S.S. Bhatnagar, J.A. Allen, and H.L. Welsh, *Can. J. Phys.* **40**, 9 (1962).

⁷A.F. Goncharov, R.J. Hemley, H.K. Mao, and J.F. Shu, *Phys. Rev. Lett.* **80**, 101 (1998).

⁸R.J. Hemley, A.F. Goncharov, H.K. Mao, E. Karmon, and J.H. Eggert, *J. Low Temp. Phys.* **110**, 75 (1998).

⁹P. Loubeyre, M. Jean-Louis, and I.F. Silvera, *Phys. Rev. B* **43**, 10 191 (1991).

¹⁰D.A. Varshalovich, A.N. Moskalev, and V.K. Khersonskii, *Quantum Theory of Angular Momentum* (World Scientific, Singapore, 1988).

¹¹J. Van Kranendonk and G. Karl, *Rev. Mod. Phys.* **40**, 531 (1968).

¹²V.G. Manzhelii, M.I. Bagatskii, I.Ya. Minchina, and A.N. Aleksandrovskii, *J. Low Temp. Phys.* **111**, 257 (1998).

¹³R.D. Ethers, R. Danilowicz, and W. England, *Phys. Rev. A* **12**, 2199 (1975).

¹⁴J. Schaefer and W. Meyer, *J. Chem. Phys.* **70**, 344 (1979).

¹⁵J. Schaefer and W.E. Köhler, *Z. Phys. D: At. Mol. Clusters* **13**, 217 (1989).

¹⁶F.H. Ree and C.F. Bender, *J. Chem. Phys.* **71**, 5362 (1979).

¹⁷I. Aviram, S. Goshen, and R. Thierberger, *J. Low Temp. Phys.* **55**, 349 (1984).

¹⁸G. Karl, J.D. Poll, and L. Wolniewicz, *Can. J. Phys.* **53**, 1781 (1975).

¹⁹J. Van Kranendonk, *Can. J. Phys.* **38**, 240 (1960).

²⁰R.J. Hemley, H.K. Mao, and J.F. Shu, *Phys. Rev. Lett.* **65**, 2670 (1990).

²¹A.F. Goncharov, V.V. Struzhkin, R.J. Hemley, H.K. Mao, and Z.X. Liu, in *Science and Technology of High Pressure*, edited by M.H. Manghnani *et al.* (Universities Press, Hyderabad, India, 2000), p. 90.

²²R.J. Hemley, H.K. Mao, L.W. Finger, A.P. Jephcoat, R.M. Hazen, and C.S. Zha, *Phys. Rev. B* **42**, 6458 (1990).

²³P. Loubeyere, R. LeToullec, D. Häusermann, M. Hanfland, R.J. Hemley, H.K. Mao, and L.W. Finger, *Nature (London)* **383**, 702 (1996).

²⁴S.N. Ishmayev, I.P. Sadikov, A.A. Chernyshov, B.A. Vindryaevskii, V.A. Sukhoparov, A.S. Telepnev, and G.V. Kobelev, *Zh. Eksp. Teor. Fiz.* **84**, 394 (1983) [*Sov. Phys. JETP* **57**, 228 (1983)].

²⁵J. Igarashi, *J. Phys. Soc. Jpn.* **53**, 2629 (1984).

²⁶Yu.A. Freiman (private communication).